

# The role of secular resonances on trojans of the terrestrial planets

R. Brasser<sup>1</sup>★ and H. J. Lehto<sup>1,2</sup>★

<sup>1</sup>*Tuorla Observatory, University of Turku, FIN-21500 Piikkiö, Finland*

<sup>2</sup>*Department of Physics, University of Turku, FIN-20014 Turku, Finland*

Accepted 2002 March 22. Received 2002 March 21; in original form 2001 November 29

## ABSTRACT

We investigate the role of secular resonances on the motion of terrestrial-planet trojans in tadpole motion for 5 Myr in the inclination range  $i \leq 90^\circ$ . We use a Fourier spectrum of the eccentricity vector,  $\mathbf{e}$ , and angular momentum vector,  $\mathbf{L}$ . When  $i > 40^\circ$ , the trojans are in a Kozai resonance with Jupiter, which increases the eccentricity to planet-crossing values on a time-scale of 0.1 Myr; hence we found no stable trojan motion when  $i > 40^\circ$ . Trojans of Mercury are unstable for a large range in inclination due to the resonances  $\nu_1$ ,  $\nu_{12}$  and  $\nu_5$ , and only those with low and high inclinations survived in our simulations. For Venus and Earth trojans, the  $\nu_3$  and  $\nu_4$  secular resonances with the Earth and Mars respectively increase the eccentricity to planet-crossing values for moderate inclinations. Venus trojans are also affected by the  $\nu_{11}$  resonance with Mercury at high inclinations hence Venus and Earth trojans are stable only at low inclinations. Mars trojans are affected by the  $\nu_3$ ,  $\nu_4$ ,  $\nu_{13}$  and  $\nu_{14}$  resonances with the Earth and Mars for low inclinations which increase the eccentricity and suppress oscillations of the inclination. At  $i = 32^\circ$ , the  $\nu_5$  resonance destabilizes Mars trojans, although its width is less than a degree in inclination. The typical lifetime of inner-planet trojans trapped in a secular resonance is 1 Myr for Venus, Earth and Mars trojans, while it is  $10^5$  yr for Mercury trojans. Trojans in secular resonances are chaotic on time-scales of  $10^3 - 10^4$  yr for all inner planets, while outside the resonances this becomes typically  $10^6$  yr.

**Key words:** celestial mechanics – minor planets, asteroids – Solar system: general.

## 1 INTRODUCTION

The motion of trojan asteroids or satellites and their stability have been investigated many times in the past since the discovery of the first Jupiter trojan, 588 Achilles, in 1906, the first trojan satellites in the Saturn system, and recently five Mars trojan asteroids, of which 5261 Eureka was the first to be discovered (Mikkola et al. 1994). There have been many numerical- and analytical studies on hypothetical trojan asteroids of the major planets (e.g. Mikkola & Innanen 1990, 1994, 1995; Érdi 1996; Tabachnik & Evans 2000; Morais 1999, 2001) which suggest that most planets can have stable trojan clouds under certain conditions. A special case of trojan motion was discovered by Michel (1997), who reported the overlapping of the  $\nu_{13}$  and  $\nu_{14}$  secular resonances in a Venus horseshoe orbit. He found that even though the inclination of the test particle increased secularly, it suffered no close approaches for a few Myr. In this study, however, we concentrate on locating any secular resonances that might destabilize the motion on short time-scales. Morais (1999) developed a secular theory for trojan motion in the elliptic restricted three-body problem up to second order in

eccentricities  $e$  and inclinations  $i$ , and calculated the free precession frequencies of the trojan. Morais (2001) uses a Hamiltonian approach to calculate the secular evolution of trojan orbits. She finds which are the secular resonances that should affect low-inclination, low-eccentricity trojans of the major planets. Her theory could be improved somewhat by using  $2 \sin \frac{i}{2}$  instead of  $i$ . Namouni & Murray (2000) developed an averaged theory up to fourth order in eccentricities and inclinations in the circular restricted three-body problem, but it is valid only for small  $i$  and moderate  $e$ . They obtained the displacement of the minima of the averaged potential from the classical Lagrangian points as a function of  $e$  and  $i$ , and calculated the secular evolution of eccentricity and pericentre. Namouni (1999) makes a classification of high-inclination, high-eccentricity orbits in a 1:1 resonance, and concludes that such orbits can provide protection mechanisms against close approaches if the argument of the pericentre librates. He finds islands of stability where motion is free from close approaches with neighbouring planets. Érdi (1996, and references therein) has done extensive work on the motion of Jupiter's trojans in the framework of the restricted three-body problem, and has established series expansion solutions of the orbital elements as a function of time. Tabachnik & Evans (1999) have studied the

★E-mail: brasser@astro.utu.fi (RB); hlehto@astro.utu.fi (HJL)

stability of Martian trojans, and have created maps that show where such trojans could safely orbit as a function of inclination and mean longitude difference between the trojan and Mars as well as mutual inclination. In a later work, Tabachnik & Evans (2000) have done extensive numerical simulations of hypothetical trojans of the inner planets, and have mapped the regions of stable motion as functions of semimajor axis  $a$ , eccentricity  $e$ , inclination  $i$  and longitude difference  $\lambda_r$ . In Section 2 we briefly explain our methods. In Section 3 we present our results, and in Section 4 we briefly comment on chaos. Conclusions follow in Section 5.

## 2 METHOD

We used the JPL Planetary and Lunar Ephemerides DE405 as initial conditions for the Solar system. To generate the ephemerides of the test particles, we take the vectors of the parent planet from the ephemerides and rotate these  $\pm 60^\circ$  around the total angular momentum vector of the Solar system. We have set the values of semimajor axis  $a$  and eccentricity  $e$  of the test particles to be the same as that of the parent planet, and have modified only their inclination  $i$  with respect to the parent planet's orbit. We deliberately chose not to modify semimajor axis and eccentricity, because forced oscillations of the eccentricity will persist anyway and will not significantly affect the locating of secular resonances since trojans with moderate or large eccentricity – ( $e > 0.35$  except in the case of Mercury) will experience a close approach with a nearby planet and be ejected from the trojan region. Tabachnik & Evans (2000) have already mapped regions of stable motion as a function of  $a$  and  $e$ . We have included the effects of all the planets except Pluto, and have simulated the system using the Wisdom–Holman algorithm (Wisdom & Holman 1991) with a time-step of 7 days (but two days for Mercury's trojans) for 5 Myr, as this proved a reasonable compromise between CPU time and the time taken for the strongest resonances to affect the dynamics significantly. We tested the validity of the code by changing the step size and comparing the generated orbital elements with earlier simulations that can be found in the literature (e.g. Murray & Dermott 1999). We found that a step size of 5 days produced a large increase in the eccentricity of the Earth, up to 0.15, which is most likely due to step size resonance. A much larger step size (Mikkola & Innanen 1994 take 22 days for Mars trojans) was too large to compute the motion of Mercury accurately. Hence we settled for a step size of 7 days. We then fed the components of the eccentricity vector  $e$ , given by

$$e = \frac{\mathbf{v} \times (\mathbf{r} \times \mathbf{v})}{GM_\odot} - \frac{\mathbf{r}}{r}, \quad (1)$$

**Table 1.** Fundamental frequencies of the Solar system, adapted from analytical solutions by Brétagneon (1974). The nodes of Jupiter and Saturn precess at the same rate.

Planet	$g_i$ ( $''\text{yr}^{-1}$ )	$s_i$ ( $''\text{yr}^{-1}$ )
Mercury	5.109	−5.611
Venus	7.346	−6.771
Earth	17.221	−18.830
Mars	17.857	−17.819
Jupiter	4.207	−26.267
Saturn	26.217	−26.267
Uranus	3.065	−2.999
Neptune	0.668	−0.691

and the angular momentum vector  $\mathbf{L}$ , through a Fourier analysing program called CLEAN (Clark 1980), which returned all fitted frequencies with their corresponding pseudo-power and phase, and compared our precession rates to those in the literature (Brétagneon 1974; Laskar 1990). We use Brétagneon's notation; thus  $g_i$  are the eigenfrequencies of the perihelia of the Solar system, and  $s_i$  are the eigenfrequencies of the nodes (see Table 1). Subscript 1 stands for Mercury and subscript 8 for Neptune, respectively. A secular resonance occurs when the free precession rate of a test particle is equal to that of one or more of the eigenfrequencies of the Solar system (Murray & Dermott 1999). A secular resonance is labelled  $\nu_i$  when  $\dot{\varpi} = g_i$  and  $\nu_{1i}$  when  $\dot{\Omega} = s_i$ .

## 3 RESULTS

Table 1 lists the fundamental frequencies of the Solar system, derived from Brétagneon (1974). We find that our values of  $g_6$  and  $s_2$  differ from those of Brétagneon's analytical solution, but are similar to those obtained by Laskar's (1990) numerical solutions. In order to demonstrate the CLEAN program, we present here an example spectrum of the eccentricity vector of the planet Mars over a 5-Myr simulation. We have chosen this for the following reasons: first, Mars has both a higher eccentricity and a higher inclination than average, so that its node and perihelion are well defined; secondly, it has some clear fourth-order effects in its spectrum. Our CLEAN program returns a fitted frequency with its corresponding pseudo-power and phase. In Table 2 we list the frequencies  $f_i$ , maximum powers  $P_i$ , and phases  $\phi_i$  of  $e_x$  for Mars. The last column states the combination of eigenfrequencies that produce the frequency in the first column in the expansion of the disturbing function (see Brétagneon 1974). The spectrum for  $e_y$  is the same as that of  $e_x$ , but with a phase shift of  $-90^\circ$ . In Table 3 we list the terms for  $e_z$ . The amplitudes can be obtained by  $A_i = 2\sqrt{P_i}$ . By comparing our results to those in Brétagneon's table 12, we find that the three strongest fourth-order effects on the eccentricity vector of Mars are, from strongest to weakest, the terms containing  $g_4 + s_3 - s_4$ ,  $g_3 - s_3 + s_4$  and  $g_4 - s_3 + s_4$  in the expansion of the disturbing

**Table 2.** Spectrum output of the Fourier analysing program of  $e_x$  for Mars. Maximum power is amplified by  $10^6$  for clarity. The component  $e_y$  is obtained from  $e_x$  by making a phase shift of  $-90^\circ$ . The phases are taken at 2.5 Myr.

$f_i$ ( $''\text{yr}^{-1}$ )	$P_i \times 10^6$	$\phi_i$ ( $^\circ$ )	Term in disturbing function
4.248	104.105	−68.99	$g_5$
7.324	2.232	37.67	$g_2$
16.749	61.352	−86.43	$g_4 + s_3 - s_4$
17.192	329.410	41.63	$g_3$
17.854	564.285	19.31	$g_4$
18.343	42.379	−18.33	$g_3 - s_3 + s_4$
18.986	5.314	−47.93	$g_4 - s_3 + s_4$
28.243	11.567	−11.99	$g_6$

**Table 3.** Spectrum output of the Fourier analysing program of  $e_z$  for Mars. Maximum power is amplified by  $10^6$  for clarity. Phases are taken at 2.5 Myr.

$f_i$ ( $''\text{yr}^{-1}$ )	$P_i \times 10^6$	$\phi_i$ ( $^\circ$ )	Term
34.874	1.470	16.54	$g_4 - s_4$
35.577	2.869	−4.29	$g_3 - s_3$

function. Comparing the amplitudes in Brétagnon's tables 10 and 12 to those in Table 2 here, we find that the greatest discrepancy is about 7 per cent in the influence of Jupiter, about 10 per cent in the value of  $g_6$ , and 6 per cent in the value of  $s_2$ . Following Brétagnon, the solution for the eccentricity of Mars, up to and including fourth-order effects would be

$$e e^{i\varpi} = \sum_{i=2}^6 A_i e^{i(g_i t + \phi_i)} + A_{41} e^{i[(g_4 + s_3 - s_4)t + \phi_{41}]} + A_{42} e^{i[(g_3 - s_3 + s_4)t + \phi_{42}]} + A_{43} e^{i[(g_4 - s_3 + s_4)t + \phi_{43}]} \quad (2)$$

From equation (2) it is apparent that the eccentricity vector of Mars is a superposition of eight sinusoid waves of different amplitudes and frequencies. Morais (2001) gives the solution for the motion of a trojan asteroid in a low-inclination, low-eccentricity orbit perturbed by other bodies. From her solutions, a secular resonance involving the longitude of perihelion,  $\varpi$ , causes the eccentricity to oscillate with large amplitude, and the orbit to precess with a frequency equal to the resonating frequency. Similarly, a secular resonance involving the longitude of the node,  $\Omega$ , causes large-amplitude oscillations of the inclination.

Since trojans with inclinations larger than  $40^\circ$  are in a Kozai resonance with Jupiter (Kozai 1962) and have typical short lifetimes of 0.1 Myr, we will concentrate the rest of our work on those trojans with  $i \leq 40^\circ$ .

### 3.1 Mercury

Mercury trojans are inherently very unstable. Tabachnik & Evans

(2000) found only a few survivors of their Mercury trojan sample, and even those might be questionable.

There are three secular resonances that act on Mercury trojans. These are the  $\nu_1$ ,  $\nu_5$  and  $\nu_{12}$  resonances. These resonances act for inclinations up to  $i = 35^\circ$ . The short lifetime of these bodies makes a determination of the locations of these resonances difficult. For low inclinations the  $\nu_1$  and  $\nu_{12}$  resonances act, while the  $\nu_5$  resonance is active for moderate inclinations ( $i \geq 20^\circ$ ). Morais (2001) already noted that the  $\nu_{12}$  resonance could affect Mercury trojans with low inclinations in small-amplitude horseshoe motion. Hence it shows in our tadpole region at moderate inclinations.

The reason Mercury trojans with vanishing inclinations may be unstable too is because the forced inclination oscillations due to perturbations of the other planets increase the inclination periodically to values that are within the  $\nu_1$  resonance or, more importantly, within the  $\nu_{12}$  resonance. Hence low-inclination Mercury trojans are drawn towards these secular resonances. This mechanism also occurs for trojans of the other inner planets, and particularly those of Mars. In Fig. 1 we plot the evolution of a low-inclination Mercury trojan to illustrate this process. We have deliberately chosen a particle that survives our integration to better illustrate these effects: the trojan gets caught in the  $\nu_{12}$  secular resonance with Venus, characterized by liberation of the argument  $\Omega - s_2 t$  as shown in the top-right panel, which increases its inclination to a value so large that it gets caught in the  $\nu_1$  secular resonance with Mercury (bottom-right panel), which increases its eccentricity. If the starting inclination of the trojan had been higher, the trojan would immediately suffer the consequences of the  $\nu_1$  and  $\nu_{12}$  resonances.

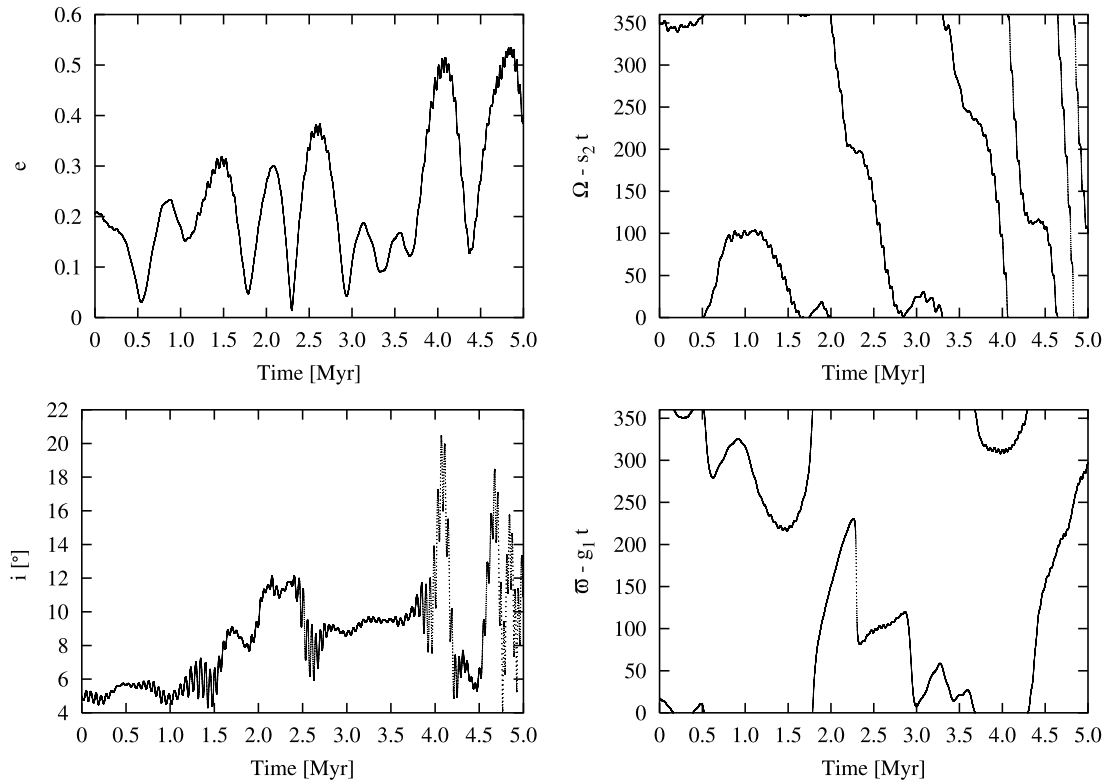


**Figure 1.** The evolution of a Mercury trojan with a starting inclination of  $i = 5^\circ$ . The top-left panel shows the evolution of the eccentricity versus time; the bottom-left panel is the inclination versus time. The top-right panel shows the argument  $\Omega - s_2 t$ , and the bottom-right panel the argument  $\varpi - g_1 t$ , the arguments of the  $\nu_{12}$  and  $\nu_1$  secular resonances. Note that frequently the above arguments are stationary, and this is responsible for increases in eccentricity and inclination.

### 3.2 Venus

Venus is one of the best planetary candidates in the inner Solar system that could harbour undiscovered trojans. In Fig. 2 we plot the amplitudes of the frequencies  $g_2 - g_5$  as a function of inclination of the  $x$ -component of the vector  $e$ . Amplitudes have been multiplied by  $10^4$  for clarity. For increasing inclination, the free precession of the asteroids decreases until at some value of  $i$  it precesses at the same rate as one of the eigenfrequencies of the Solar system, which is the condition for a secular resonance to occur (Murray & Dermott 1999). The *free* eccentricity and inclination are defined as the fundamental orbital parameters of the particle derived from its boundary conditions (Murray & Dermott 1999). In contrast, the *forced* eccentricity and inclination are determined solely by the value of the semimajor axis and the secular solution of the perturbing bodies. The free precession for low-eccentricity, low-inclination trojans is approximately given by (Morais 1999)

$$\gamma = \frac{27}{8} \mu_1 n_1, \quad (3)$$

where  $\mu_1$  is the planet/Sun mass ratio, and  $n_1$  is the mean motion of the planet.

In Fig. 2 we see, as expected, that the secular resonances cause large-amplitude oscillations of the eccentricity, with  $g_4$  being stronger for lower inclinations and  $g_3$  for larger inclinations.

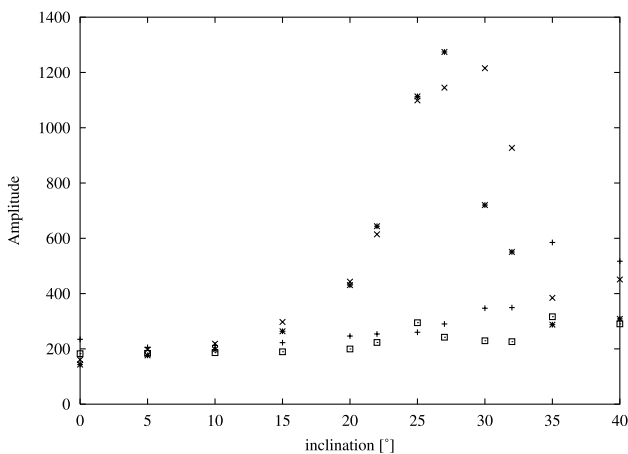


**Figure 2.** The amplitudes of the frequencies  $g_2 - g_5$  of  $e_x$  on Venus trojans. The amplitude of  $g_2$  is shown by +,  $g_3$  by  $\times$ ,  $g_4$  by \*, and  $g_5$  by  $\square$ .

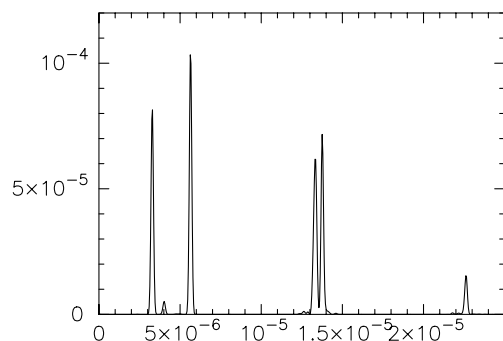


**Figure 3.** Spectrum of  $e_x$  of a Venus trojan at  $i = 4^\circ$ . The ordinate is the frequency, while the abscissa is the pseudo-power of the CLEANED peak. The main peaks are, from left to right, caused by Jupiter, Mercury (small), and Venus, Earth, Mars and Saturn.

Tabachnik & Evans (2000) report that no Venus trojans survived their 75-Myr integration with  $i > 16^\circ$ . Since our integration lasted only 5 Myr, we cannot confirm this statement. However, we find that the  $\nu_3$  and  $\nu_4$  secular resonances act in the region  $17^\circ$  to  $35^\circ$ , so

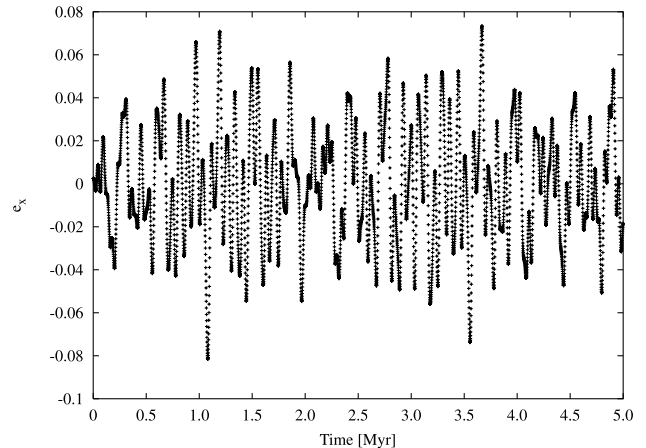


**Figure 4.** The evolution of  $e_x$  for a Venus trojan at  $i = 4^\circ$ . The plot is a superposition of six waves, whose components are given in Fig. 3.

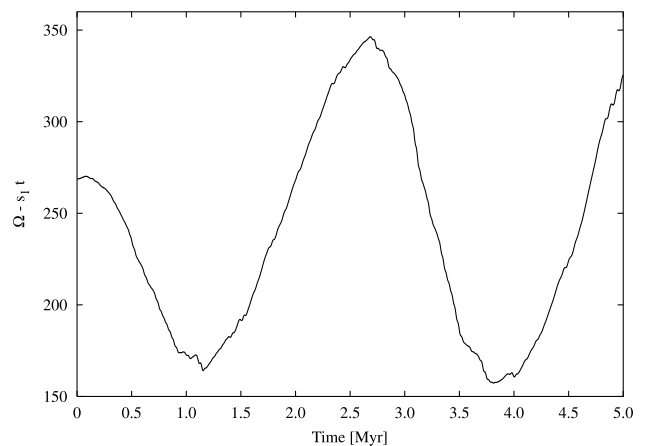


**Figure 5.** Plot of the argument  $\Omega - s_1 t$  of a Venus trojan in the  $\nu_{11}$  resonance with Mercury. Note the large libration amplitude.

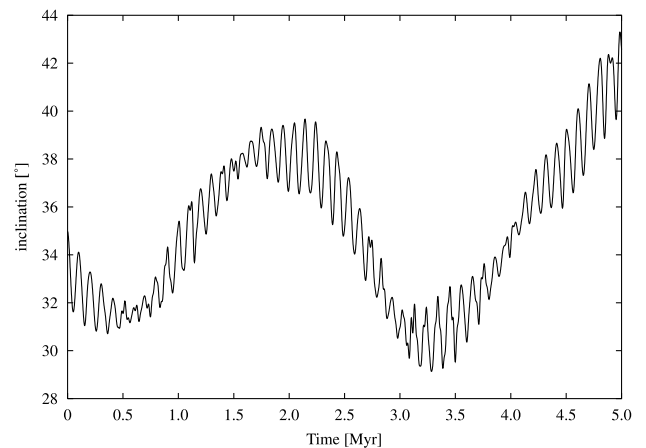


**Figure 6.** Plot of the inclination of a Venus trojan in the  $\nu_{11}$  resonance with Mercury. Long-period oscillations of the inclination are out of phase with the argument  $\Omega - s_1 t$  by  $90^\circ$ , and have the same frequency as librations of  $\Omega - s_1 t$ .

that Venus trojans cannot exist in this region of phase-space. Note that these secular resonances are dangerous for the trojan only if it increases the eccentricity up to values that make it Earth-crossing. Even though for  $i = 15^\circ$  the amplitudes of  $g_3$  and  $g_4$  are significantly larger than  $g_2$  and  $g_5$ , the influence is still too weak to make the trojan Earth-crossing. Fig. 3 is an example of a CLEANED spectrum and shows the frequencies of  $e_x$  of a Venus trojan at  $i = 4^\circ$ . The peaks are caused by Jupiter (left), Mercury (small), and Venus, Earth, Mars and Saturn (right). Fig. 4 shows the evolution of  $e_x$  as a function of time, which is a wavelet output of the spectrum showed in Fig. 3 and is of the form

$$e_x e^{i\varpi} = \sum_{i=1}^6 A_i e^{i(g_i t + \phi_i)}. \quad (4)$$

At high inclinations, from  $32^\circ$  to  $38^\circ$ , the  $\nu_{11}$  resonance affects Venus trojans. We found that the argument  $\Omega - s_1 t$  is not constant, but librates with large amplitude and a period of around 2.5 Myr. An example of this argument is shown in Fig. 5, while Fig. 6 shows the corresponding behaviour of the inclination. The large-amplitude oscillations of the inclination are out of phase by  $90^\circ$  with those of the argument  $\Omega - s_1 t$ , and have the same frequency.

### 3.3 Earth

Tabachnik & Evans (2000) reported Earth-trojan instability at inclinations ranging from  $16^\circ$  to  $25^\circ$ . We noted that for  $i = 27^\circ$  there is a large peak in the spectrum of  $e$  when  $\dot{\varpi} = 2g_2$ , but this did not seem to affect the magnitude of the eccentricity during our simulation. At  $i \sim 40^\circ$  a secular resonance with Venus occurs, the  $\nu_2$  resonance, although this width of the resonance is rather small. Besides, trojans with  $i \geq 40^\circ$  are affected by the Kozai resonance (Kozai 1962) with Jupiter, so that those become Venus-crossing on a time-scale of  $10^5$  yr. Morais (2001) already found that the resonances  $\nu_3$  and  $\nu_3$  can affect Earth trojans. Fig. 7 shows a plot of the amplitudes of the eigenfrequencies  $g_2 - g_5$  on Earth trojans. Amplitudes have been magnified by a factor of  $10^4$  for clarity. We find that Earth trojans are unstable for inclinations ranging from  $12^\circ$  up to  $25^\circ$ , which is a slightly larger range than that determined by Tabachnik & Evans (2000).

Wiegert, Innanen & Mikkola (1997) found that asteroid 3753 Cruithne is a temporary Earth-trojan in a peculiar horseshoe orbit with the opening not centred around the Earth, but with some

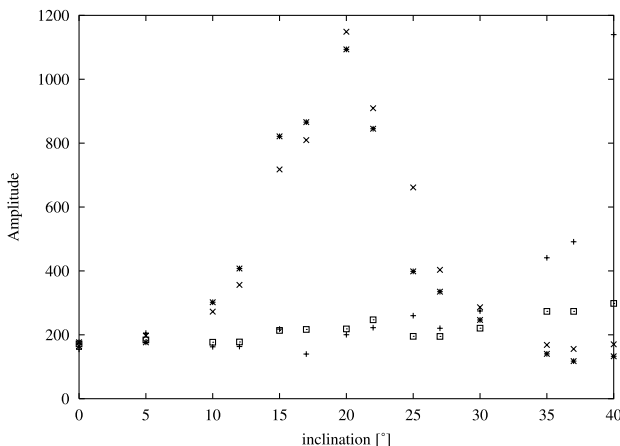


**Figure 7.** The amplitudes of the frequencies  $g_2 - g_5$  on  $e_x$  of Earth trojans. The amplitude of  $g_2$  is shown by +,  $g_3$  by x,  $g_4$  by \*, and  $g_5$  by □.

offset. Recently, Chodas et al. (2002) found two more such asteroids in temporary horseshoe motion with the Earth, with lifetimes of a few thousand years. This implies that there could be stable trojan motion with the Earth on short time-scales, and hence that it is likely that there might be more undiscovered (temporary) Earth trojans. Whiteley & Tholen (1998) have made an active search for these objects. They covered an area of  $0.35 \text{ deg}^2$  to a limiting sensitivity of  $R \sim 22.8$ . Since no objects were found, this led them to conclude that the number of objects at or above their detection threshold is  $\leq 3$  per square degree.

### 3.4 Mars

The qualitative behaviour of Mars trojans has been thoroughly investigated by Mikkola & Innanen (1994) and by Tabachnik & Evans (2000). The dynamics of Mars trojans is completely different from that of Venus and Earth trojans. Mikkola & Innanen (1994) report that the argument  $2\dot{\varpi} + \dot{\Omega} - g_5$  is zero in the inclination range  $11^\circ$  to  $16^\circ$  with respect to the orbit of Mars, and this is verified by Tabachnik & Evans (2000). In our simulations we have been unable to verify this statement. Mikkola & Innanen (1994) used a coordinate system rotating with the perihelion of Mars in one case and with the perihelion of Jupiter in another case, while we use a fixed-axes coordinate system. Hence their fig. 5 plots  $\dot{\Omega} + s_4$  and  $\dot{\varpi} - g_4$  instead of  $\dot{\Omega}$  and  $\dot{\varpi}$ . In their fig. 6 the rates are  $\dot{\Omega} - g_5$  and  $\dot{\varpi} - g_5$ . In our fixed-axes coordinate system the resonance  $2\dot{\varpi} + \dot{\Omega} - g_5$  found by Mikkola & Innanen (1994) becomes  $2\dot{\varpi} + \dot{\Omega} - 3g_5$ . This is a high-order resonance, and we have not found this resonance to affect the dynamics of Mars trojans.

Instead, we found that the dynamics of low-inclination Mars trojans is governed by four resonances: the  $\nu_3$  and  $\nu_4$  resonances with the Earth and Mars for inclinations up to  $12^\circ$ , and the  $\nu_{13}$  and  $\nu_{14}$  resonances for inclinations up to  $13^\circ$ ; see Fig. 8, which is a plot of the rates  $\dot{\Omega} + s_{3,4}$  versus inclination in the top panel, and  $\dot{\varpi} - g_{3,4}$  versus inclination in the bottom panel. For a large range in inclination all arguments are (near)zero, meaning that the said trojans are in secular resonance. We found no difference whether the trojans were situated at  $L_4$  or  $L_5$ . These resonances are much stronger than the high-order resonance with Jupiter. Morais (2001) shows that the  $\nu_4$ ,  $\nu_{13}$  and  $\nu_{14}$  resonances affect Mars trojans, but does not find the  $\nu_3$  resonance to play any role. For  $i \geq 15^\circ$ , the amplitudes of the free components of the eccentricity and inclination of the trojan are at least an order of magnitude larger than those induced by the planets. In Fig. 9 we plot the amplitudes of the modes  $g_3 - g_5$  for Mars trojans. We notice that amplitudes are largest for inclinations ranging from  $4^\circ$  to  $12^\circ$ , which is the range at which Tabachnik & Evans (2000) found the resonance  $2\dot{\varpi} + \dot{\Omega} - g_5$  with Jupiter to be strongest. We believe that this is not the case, and that the stated secular resonances with the Earth and Mars are responsible.

## 4 CHAOS

By calculating the Lyapunov exponent of all trojans, we obtained some typical time-scale for chaos to set in. Mikkola & Innanen (1994) found that for Mars trojans instability occurs suddenly. We found the same to be true for all trojans of the inner planets caught in secular resonances. The sudden increase in  $\ln|dr|$  is due to a close approach with another planet (see Mikkola & Innanen 1994). The sooner this occurs, the shorter the typical Lyapunov time and lifetime of the trojan. The latter quantity is obtained by



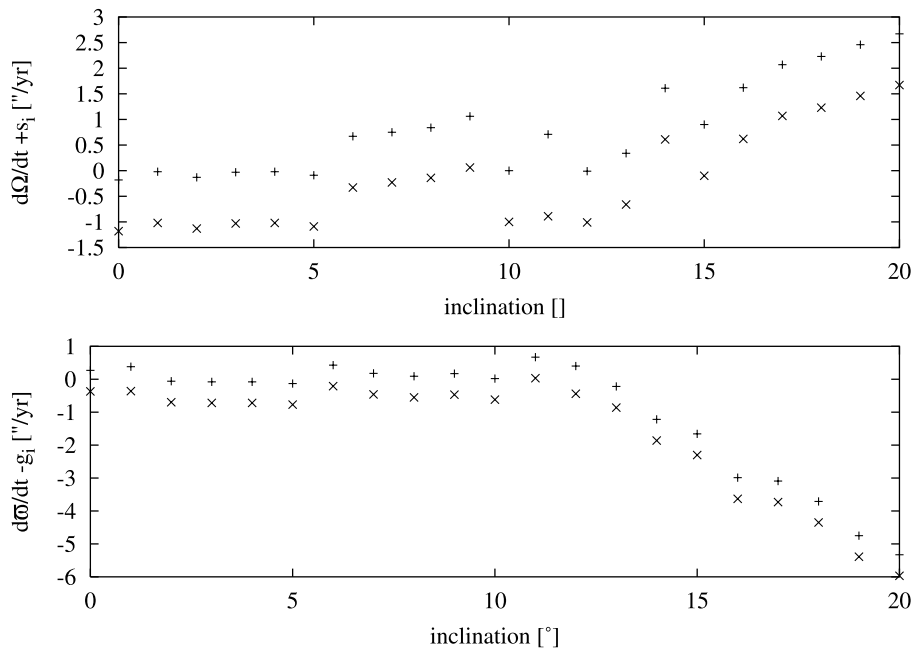


**Figure 8.** A plot of the arguments  $\dot{\Omega} + s_{3,4}$  versus inclination in the top panel, and  $\dot{\varpi} - g_{3,4}$  versus inclination in the bottom panel. Arguments with the Earth ( $g_3, s_3$ ) are marked with +, while those with Mars ( $g_4, s_4$ ) are marked with  $\times$ . Note that for a large range in inclination all arguments are near zero, so that the trojans are in secular resonance.

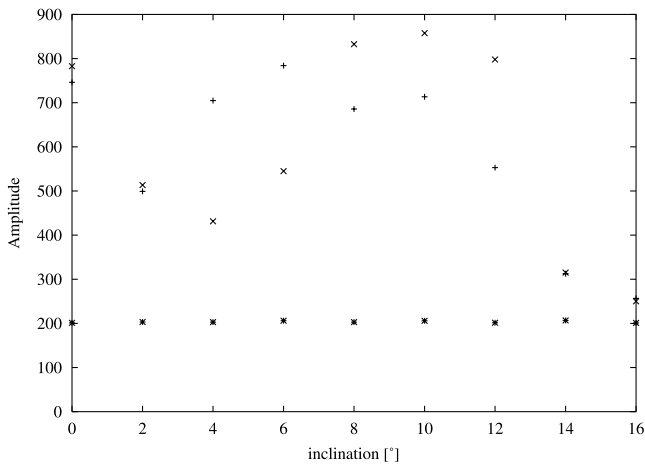


**Figure 9.** The amplitudes of the frequencies  $g_3 - g_5$  on  $e_x$  of Mars trojans. The amplitude of  $g_3$  is shown by +,  $g_4$  by  $\times$ , and  $g_5$  by \*. Amplitudes are multiplied by  $10^4$  for clarity.

simultaneously integrating the difference equations together with the equations of motion. This allows us to keep track of the divergence of any neighbouring trajectories. Fig. 10 shows the obtained Lyapunov times as a function of inclination for trojans of each planet. The values were obtained before a close approach with a planet occurred during the simulation, if any, so that the chaos inherent of the orbit is obtained and not the chaos due to successive close approaches with the inner planets. For Mercury trojans, the Lyapunov time decreases with increasing inclination. The single dot for  $i = 13^\circ$  is due to the very short lifetime of the trojan. The typical lifetime of Mercury trojans in the  $\nu_1, \nu_{12}$  and  $\nu_5$  secular resonances is 0.1 Myr. High-inclination Mercury trojans, though having shorter Lyapunov times, have average lifetimes of 1 Myr. For Venus and Earth trojans we conclude that particles trapped within the  $\nu_3$  and  $\nu_4$  resonances are chaotic on

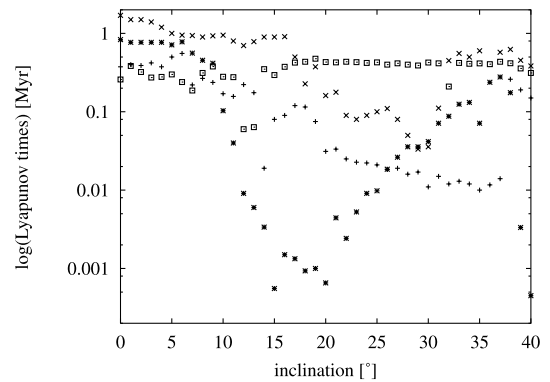


**Figure 10.** The Lyapunov times of trojans of the inner planets as a function of inclination. The Mercury trojans are shown by +, those of Venus by  $\times$ , Earth trojans by \*, and Mars trojans by  $\square$ .

time-scales of  $10^3$  yr for the Earth and  $10^4$  yr for Venus. For particles outside these resonances, the Lyapunov time increases to typically 1.5 Myr for Venus trojans and 1 Myr for Earth trojans for low inclinations, and to 0.7 Myr for high inclinations. The typical lifetime for Venus and Earth trojans in the resonances is 1 Myr. For Mars, Lyapunov times of trojans caught in the secular resonances with the Earth and Mars are 0.3 Myr, while for trojans in the stable region this increases to typically 0.4 Myr, which is in agreement with Mikkola & Innanen (1994). Note the single lower dot for  $i = 32^\circ$ , which is caused by the  $\nu_5$  resonance with Jupiter. The two dots at  $i = 12^\circ$ , and  $13^\circ$  are due to the fact that for those inclinations the  $\nu_{13}$  and  $\nu_{14}$  resonances are strongest. Even though the chaotic time-scales of Mars trojans in the region free of secular resonances are shorter than those of Venus and Earth trojans, this does not necessarily affect the stability of motion. By comparison, the typical Lyapunov time for an asteroid in the inner Solar system is a few hundred years (Wiegert, Innanen & Mikkola 1998).

**Table 4.** Secular resonances affecting trojans of the inner planets.

Planet	Affecting resonances	Inclination range [°]
Mercury	$\nu_1, \nu_{12}, \nu_5$	0–35
Venus	$\nu_3, \nu_4$	17–35
Venus	$\nu_{11}$	32–38
Earth	$\nu_3, \nu_4$	12–30
Mars	$\nu_3, \nu_4, \nu_{13}, \nu_{14}$	0–11
Mars	$\nu_5$	32

## 5 CONCLUSIONS

We have shown that the stability of trojans in tadpole motion of the inner planets is governed by secular resonances. The resonances involving the longitude of pericentre,  $\nu_i$ , increase the eccentricity of the trojan up to planet-crossing values so that it inevitably experiences a close approach with a neighbouring planet and will be ejected from the trojan cloud. The resonances with the node,  $\nu_{1i}$ , increase the inclination which can result in the trojan being captured in a resonance involving the longitude of perihelion. For Mercury, the affecting resonances are  $\nu_1$  and  $\nu_5$ , which increase the eccentricity to Venus-crossing orbits, and the  $\nu_{12}$  resonance, which increases the inclination to a value so large that the trojan gets trapped in the former resonances. For Venus and the Earth, the  $\nu_3$  and  $\nu_4$  secular resonances determine the regions of stability while Venus trojans are also affected by the  $\nu_{11}$  resonance at high inclinations. For Mars, the  $\nu_3, \nu_4, \nu_{13}$  and  $\nu_{14}$  resonances increase the eccentricity and inclination of low-inclination Mars trojans so that a close approach with the Earth will occur. Table 4 lists a summary of the secular resonances affecting trojans of the inner planets, together with their inclination range. For Mercury and Mars, the secular resonances overlap so that no clear boundary is visible for each individual resonance; hence we have stated the total inclination range affected by secular resonances. The inclination range for Venus trojans is larger than that for Earth because of the neighbouring secular resonance with Mercury. The typical lifetime of a trojan trapped in the resonances is 1 Myr for Venus, Earth and Mars trojans, while it is 0.1 Myr for Mercury trojans. Typical Lyapunov time-scales of trojans in secular

resonance is  $10^3$  yr for Earth trojans 0.3 Myr for Mars trojans. Outside these regions it is typically 0.4 Myr for Mars trojans to 1.5 Myr for Venus trojans.

## ACKNOWLEDGMENTS

We are grateful to Seppo Mikkola for providing us with the computer code of the Wisdom–Holman integrator and comments. We also thank Maria Helena Morais, Mauri Valtonen, Kimmo Innanen, Pasi Nurmi and Chris Flynn for reading the manuscript. A anonymous referee is also thanked for valuable criticism. This work was supported by grant 44011 from the Finnish Academy.

## REFERENCES

- Brétagnon P., 1974, *A&A*, 30, 141  
 Chodas P., Connors M., Mikkola S., Wiegert P., Veillet C., Innanen K., 2002, *Planet. Space Sci.*, submitted  
 Clark B. J., 1980, *A&A*, 89, 337  
 Érdi B., 1996, *Celest. Mech. Dyn. Astron.*, 65, 149  
 Kozai Y., 1962, *AJ*, 67, 591  
 Laskar J., 1990, *Icarus*, 88, 266  
 Michel P., 1997, *A&A*, 328, L5  
 Mikkola S., Innanen K., 1990, *AJ*, 100, 290  
 Mikkola S., Innanen K., 1994, *AJ*, 107, 1879  
 Mikkola S., Innanen K., 1995, *Earth, Moon, Planets*, 71, 195  
 Mikkola S., Innanen K., Muinonen K., Bowell E., 1994, *Celest. Mech. Dyn. Astron.*, 58, 53  
 Morais M. H. M., 1999, *A&A*, 350, 318  
 Morais M. H. M., 2001, *A&A*, 369, 677  
 Murray C. D., Dermott S. F., , *Solar system Dynamics*. Cambridge Univ. Press, Cambridge, New York  
 Namouni F., 1999, *Celest. Mech. Dyn. Astron.*, 137, 293  
 Namouni F., Murray C., 2000, *Celest. Mech. Dyn. Astron.*, 76, 131  
 Tabachnik S., Evans N. W., 2000, *MNRAS*, 319, 63  
 Whiteley R. J., Tholen D. J., 1998, *Icarus*, 136, 154  
 Wiegert P., Innanen K., Mikkola S., 1997, *Nat*, 387, 685  
 Wiegert P., Innanen K., Mikkola S., 1998, *AJ*, 115, 2604  
 Wisdom J., Holman M., 1991, *AJ*, 102, 152

This paper has been typeset from a  $\text{\TeX}/\text{\LaTeX}$  file prepared by the author.